JOURNAL OF COMPUTATIONAL PHYSICS 31, 113–145 (1979)

# Mixed Finite-Element Methods for Incompressible Flow Problems*

M. FORTIN

*Université Laval, Département de Mathématiques, Québec, Canada*

AND

F. THOMASSET

*IRIA–LABORIA, Rocquencourt, 78 Le Chesney, France*

Received January 20, 1978; revised April 13, 1978

This paper presents finite-element methods to approximate both inviscid and viscous incompressible flow problems. First one introduces general ideas and a scheme is presented for inviscid flow using discontinuous finite elements which allow a precise definition of upwind derivatives. It is then shown that such a scheme can be extended to viscous flow if the viscosity terms are treated through mixed finite elements. We give numerical results that show that this approach enables to compute at fairly large Reynolds number with reasonable accuracy. A complete error analysis is up to now out of reach, but we give results on model problems to get at least an intuitive view of the quality of the method proposed.

## 1. INTRODUCTION

Numerical fluid dynamics is, by no doubt, one of the most difficult topics of numerical analysis. Among the problems that are to be faced, the hardest to handle is probably to simulate efficiently the behavior of fluids when viscosity becomes small or more exactly when the Reynolds number becomes large. To fix up ideas, let us write the Navier–Stokes equations in nondimensional form for an incompressible fluid.

Let $\{u_1, u_2, u_3\}$ be the velocity vector and $p$ the static pressure. We then have to solve

$$\frac{\partial u_i}{\partial t} - \frac{1}{\mathrm{Re}} \Delta u_i + \sum_j u_j \frac{\partial u_i}{\partial x_j} + \frac{\partial p}{\partial x_i} = f_i , \tag{1.1}$$

$$\operatorname{div} u = \sum_i \frac{\partial u_i}{\partial x_i} = 0 \tag{1.2}$$

with appropriate initial and boundary conditions.

* This work was supported partly by NRC Grant A8195 and by a "Subvention FCAC" from the Ministère de l'Education du Québec.



0021-9991/79/040113-33$02.00/0

The Reynolds number Re that appears in (1.1) may generally be written in the form,

$$\mathrm{Re} = Ud/\nu, \tag{1.3}$$

where $U$ and $d$ are reference velocity and length and $\nu$ is the kinematic viscosity.

In many physically interesting situations, Re may be large (say $10^5$, for instance). For such a case, (1.1) is clearly dominated by its nonlinear hyperbolic part, except in boundary layers, where the gradient of velocity is large, thus enabling viscosity to play a role. Furthermore, large Reynolds numbers are likely to mean the appearance of turbulent solutions, which may be loosely described as unstable and to a certain extent random.

In either case, the size of the physical phenomena that are to be simulated becomes exceedingly small with respect to any possible discretization grid, even on the largest computers available and even foreseeable. Moreover, it is clear that any numerical solution that merely ignores those phenomena can only be considered as meaningless.

We shall not, in this paper, try to modelize turbulent flows. However, we shall state, in place, how our method might be adapted to such a model, at least in the frame of modeling turbulence through an additional (nonlinear) dissipative term.

We shall then try to take into account boundary layers, replacing them by discontinuities. This may be acceptable from a large-scale point of view. We shall then have to develop a numerical scheme allowing a discontinuous solution. Viscosity will then be introduced using mixed finite elements. It will act as a friction factor limiting the appearance and size of discontinuities and feeding in dissipation whenever a discontinuity develops.

## 2. Precise Problem Definition

In order to get a finite-elements approximation of flow problems, we first have to define a variational formulation for these problems. We shall treat, here, homogeneous boundary conditions, in order to avoid technical difficulties, that anyway present no problems is numerical computation. We use throughout the standard summation convention of repeated indices.

Let then $\Omega$ be a bounded domain of $\mathbf{R}^N$ ($N = 2$ or 3), with smooth boundary $\Gamma$. We want to find in $\Omega$ a velocity vector field $u = \{u_i\}$, $i = 1,..., N$, and a scalar function $p$ such that

$$\frac{\partial u_i}{\partial t} + \frac{\partial (u_i u_j)}{\partial x_j} + \frac{\partial p}{\partial x_i} = f_i + \nu \, \Delta u_i , \qquad i = 1,..., N, \tag{2.1}$$

$$\operatorname{div} u = \sum_i \frac{\partial u_i}{\partial x_i} = 0, \tag{2.2}$$

$$u_i(x, 0) = u_i^0(x), \tag{2.3}$$

$$u_i \,|_\Gamma = 0. \tag{2.4}$$

Let $n$ and $\tau$ be respectively the unit normal and tangential vectors to the boundary $\Gamma$. Condition (2.4) may be split into

$$u \cdot n_{|\Gamma} = 0, \tag{2.5}$$

$$u \cdot \tau_{|\Gamma} = 0. \tag{2.6}$$

Condition (2.6) is the so-called no-slip boundary condition for viscous flow. For inviscid flow, we have to solve Euler's equations that is (2.1) with $\nu = 0$, (2.2), (2.3), and (2.5).

We now introduce function spaces in order to write these equations in variational form. We define in a standard way (cf., e.g., Lions [16] and Teman [18]).

$$L^2(\Omega) = \left\{ v \;\middle|\; \int_\Omega | v |^2 \, dx < +\infty \right\}. \tag{2.7}$$

It is the space of a square integrable function on $\Omega$. We denote by

$$| v |^2 = \int_\Omega | v |^2 \, dx \tag{2.8}$$

the norm of a function $v$ in $L^2(\Omega)$ and by

$$(u, v) = \int_\Omega fv \, dx \tag{2.9}$$

the scalar product in $L^2(\Omega)$. Let then

$$H_0^1(\Omega) = \left\{ v \;\middle|\; v \in L^2(\Omega), \frac{\partial v}{\partial x_i} \in L^2(\Omega), i = 1,..., N, v \,|_\Gamma = 0 \right\}. \tag{2.10}$$

It can be shown that

$$\| v \|^2 = \sum_{i=1}^{N} \left| \frac{\partial v}{\partial x_i} \right|^2 \tag{2.11}$$

defines a norm on $H_0^1(\Omega)$. We shall use in the sequel vector fields $u = \{u_i\}$, $i = 1,..., N$, where each component will lie in $L^2(\Omega)$ or in $H_0^1(\Omega)$. We still denote by

$$\begin{aligned} | u |^2 &= \sum_{i=1}^{N} | u_i |^2, \\ \| u \|^2 &= \sum_{i=1}^{N} \| u_i \|^2 \end{aligned} \tag{2.12}$$

the norms of the vector in $(L^2(\Omega))^N$ and $(H_0^1(\Omega))^N$, respectively.

We now consider a space of solenoidal vector fields, of which each component belongs to $H_0^1(\Omega)$,

$$V = \{u = \{u_i\} \mid u_i \in H_0^1(\Omega),\ i = 1,\ldots, N,\ \operatorname{div} v = 0\}. \tag{2.13}$$

This will be the standard space for the velocity field when solving (2.1)–(2.4). Multiplying (2.1) by a test function $v \in V$ and integrating over $\Omega$, taking note that $\int_\Omega \operatorname{grad} pv\, dx = -\int_\Omega p \operatorname{div} v\, dx = 0$, we get

$$(u_i', v_i) + \nu \int_\Omega \frac{\partial u_i}{\partial x_j}\frac{\partial v_i}{\partial x_j}\, dx + \int_\Omega \frac{\partial u_i u_j}{\partial x_j} v_i\, dx = \int_\Omega f_i v_i\, dx, \qquad \forall v \in V, \tag{2.14}$$

$$u \in V, \tag{2.15}$$

$$u_i(x, 0) = u_i^0(x). \tag{2.16}$$

This is a weak formulation of the Navier–Stokes equations, introduced by Leray [13]. It is shown for instance in [16] that there is a unique solution to (2.14)–(2.16) for a two-dimensional problem and at least one for the three-dimensional case.

In order to get the existence of a solution for the inviscid problem, a fairly natural way would be to consider the behavior of a viscous solution when viscosity becomes small. It could be hoped that such a solution should converge to an inviscid solution. This is, up to date, an unsolved problem and some of the difficulties encountered might be related to the onset of turbulence.

Nevertheless, we shall take as granted that such a convergence occurs. It is then clear that this cannot happen in $V$ as inviscid solution do not satisfy the no-slip condition. It turns out that the natural space for inviscid solution would then be

$$H = \{u = \{u_i\} \mid u_i \in L^2(\Omega),\ i = 1,\ldots, N,\ \operatorname{div} u = 0,\ u \cdot n_{|\Gamma} = 0\}. \tag{2.17}$$

This space may in turn be imbedded in a larger space,

$$H(\operatorname{div}; \Omega) = \{u = \{u_i\} \mid u_i \in L^2(\Omega),\ i = 1,\ldots, N,\ \operatorname{div} u \in L^2(\Omega)\}. \tag{2.18}$$

It must be pointed out that if convergence to an inviscid solution ever takes place, it is because functions of $H$ that do not satisfy the no-slip condition can be approximated in the norm of $H$ (i.e., in $L^2(\Omega)$ norm) by functions of $V$ which satisfy the no-slip condition. This is not the case for standard finite-element approximations of (2.13)–(2.15), (cf. Fortin [8], Teman [18], and Crouzeix–Raviart [7] for instance), unless the mesh is indefinitely refined, that is, in no practical circumstance.

We shall then try to define approximations of (2.14)–(2.16) using $H$ as a basic space. We shall have to weaken (2.14) before we can do so. Indeed for $u \in H$, $\partial(u_i u_i)/\partial x_j$ will in general be meaningless, unless we allow for derivatives in the sense of distributions.

Before doing so, we shall consider a finite-element approximation for $H$ as our development will be made directly on a finite-element formulation.

## 3. Approximation of $H$ by Finite Elements

We shall consider almost exclusively here the two-dimensional case. It is well know that a two-dimensional solenoidal vector field may be expressed as the curl, or rotational, of a stream function $\psi$, namely,

$$u = \operatorname{rot} \psi = \left\{ \frac{\partial \psi}{\partial x_2}, -\frac{\partial \psi}{\partial x_1} \right\}. \tag{3.1}$$

It comes out that for a simply connected (i.e., without holes) domain the stream function associated to $u \in H$ belongs to $H_0^1(\Omega)$. In fact for $\psi \in H_0^1(\Omega)$, $u = \operatorname{rot} \psi \in (L^2(\Omega))^n$ and $u \cdot n_{|\Gamma} = \partial\psi/\partial\tau\,|_\Gamma = 0$. This last condition states that $\psi$ must be constant on $\Gamma$. Thus, choosing $\psi$ such that $\psi_{|\Gamma} = 0$ is just a convenient setup.

From a finite-element point of view, the above development implies that it is a fairly easy task to obtain a discrete analog of $H$. Indeed, standard conforming elements enable us to get directly an approximation of $H_0^1(\Omega)$. Then taking the curl of such an approximation provides an approximation of $H$.

Precisely, let, $\tau_h$ be a partition of $\Omega$ in triangular elements and

$$W_h^k = \{\psi_h \mid \psi_h\,|_K \in P_k(K), \forall K \in \tau_h\,,\ \psi_h \text{ continuous on } \Omega\}, \tag{3.2}$$

$$W_{0h}^k = \{\psi_h \mid \psi_h \in W_h^k,\ \psi_h\,|_\Gamma = 0\}, \tag{3.3}$$

where $P_k(K)$ is the set of polynomials of degree $k$ on the element $K$. These definitions can be translated in a standard way for quadrilateral elements. We have, of course, $W_{0h}^k \overset{c}{\hookrightarrow} H_0^1(\Omega)$. We now define

$$H_h = \{u_h \mid u_h = \operatorname{curl} \psi_h\,,\ \psi_h \in W_{0h}^k\}; \tag{3.4}$$

this is an internal approximation of $H$ (i.e., $H_h \overset{c}{\hookrightarrow} H$). In our numerical computations, we used piecewise quadratic elements ($P_2$) of standard type. We have continuity on element interfaces. Taking the curl gives out a function of $H$ which is piecewise linear ($P_1$) and for which $u \cdot n$ is continuous on interfaces. This last fact is clear as $\partial\psi/\partial\tau$ is the same from any side of element boundarier by continuity of $\psi$.

However, on the interface $S$, we may have a jump of $u \cdot \tau$, as $\partial\psi/\partial n$ is not continuous. We have already signaled that $H$ can be imbedded in a larger space $H(\operatorname{div}; \Omega)$. Finite-element approximations of this space have been considered by Raviart and Thomas [17]. They have shown that for such approximations, one must have continuity of $u \cdot n$ on element boundaries. It also turns out of their analysis that our approximations of $H$ are just the solenoidal vector fields in their approximation of $H(\operatorname{div}; \Omega)$. From this analysis it turns out that if we want to compute pressure (that disappears in (2.14)) it will be a discontinuous piecewise linear function.

It is also possible to consider quadrilateral elements, and we shall see later that there might be some advantage to do so from the point of view of error analysis. If, for instance, we use a bilinear approximation ($Q_1$) for $\psi$ on rectangles, it is an easy thing to see that we get back the MAC cell for the discretization of $u$.

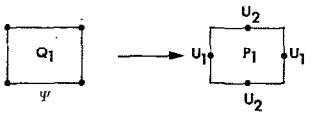


*Remark* 3.1. For a domain with holes (flow around a body), we only know that $\psi$ is constant on every connected component of the boundary. If we fix up an arbitrary value of $\psi$ on $\Gamma_0$, the value on $\Gamma_1$ is then an unknown of the problem. Numerically we define an extra basis function for the discrete stream function $\psi_h$, such that $\psi_h = 1$ at every node on $\Gamma_1$ and $\psi_h = 0$ for other $n$ nodes. We shall come back to this point.

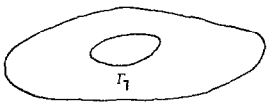


*Remark* 3.2. In a three-dimensional problem it is no longer possible to use stream functions to define a solenoidal vector field, at least in a one-to-one way. Thus we have to use directly a discretization of $H(\text{div}; \Omega)$ and consider the subspace of solenoidal fields. It is a simple exercise to verify that the constructions of Raviart and Thomas can be extended to three-dimensional cases. Although a numerical study remains to be done, there is no theoretical reason why the techniques developed here should be limited to a two-dimensional model.

## 4. A Discrete Formulation for Euler Equations

We shall use here some ideas developed by Lesaint [14] for the approximation of linear hyperbolic problems. (See also Lesaint–Raviart [15]). An interesting feature of the scheme is the use of upwind derivatives which stick to the hyperbolic nature of the problem. The ideas developed here have been already presented in Fortin [9] and Thomas–Set [19].

We have in fact to deal with the nonlinear convective terms. Let then $K$ be an element of the discretization considered and let us write

$$\int_K \frac{\partial}{\partial x_j}(u_i u_j)\, v_i \, dx = -\int_K (u_i u_j) \frac{\partial v_i}{\partial x_j} dx + \int_{\partial K} u \cdot n (u_i v_i)\, d\sigma. \tag{4.1}$$

The basic idea of Lesaint's method is to split $\partial K$ into two parts.

$\partial K_-$ is the part of $\partial K$ where $u \cdot n < 0$, that is, $\partial K_-$ is upwind of $K$.
$\partial K_+$ is the part of $\partial K$ where $u \cdot n > 0$, that is, $\partial K_+$ is downwind of $K$.

Let us remark that as $u \cdot n$ is continuous on interfaces, the definition of $\partial K_+$ *is*

*consistent from one element to another.* Let us consider two triangles (for instance) which share a side $S$. We then define on $S$

$$u^+|_S \text{ is the downwind value of } u \text{ on } S,$$
$$u^-|_S \text{ is the upwind value of } u \text{ on } S,$$

or precisely on an element $K$.

$$u|_{\partial K} = \begin{cases} u^+ \text{ on } \partial K_+ , \\ u^- \text{ on } \partial K_- . \end{cases} \tag{4.2}$$

On $S$ we then have two values of $u$, $u^+$ and $u^-$. Following Lesaint, we then write as a variational formulation for Euler equations

$$(u', v) - \sum_K \left( \int_K (u_i u_j) \frac{\partial v_i}{\partial x_j} \, dx - \int_{\partial K} u \cdot n (u_i^+ v_i) \, d\sigma \right) = \int_\Omega f_i v_i \, dx, \qquad \forall v \in H_h ,$$
$$u \in H_h . \tag{4.3}$$

Integrating again by part the nonlinear term in (4.3), we obtain, using the definition of $u^+$ and $u^-$,

$$(u', v) + \sum_K \left( \int_K \frac{\partial}{\partial x_j} (u_i u_j) \, v_i \, dx + \int_{\partial K_-} u \cdot n [u_i] \, v_i \, d\Gamma \right) = \int_\Omega f_i v_i \, dx,$$
$$[u_i]|_{\partial K} = u_i^{\text{ext}} - u_i^{\text{int}} = \text{jump of } u_i \text{ on } \partial K. \tag{4.4}$$

Here $u_i^{\text{ext}}$ and $u_i^{\text{int}}$ evidently denote on $\partial K$ the value of $u$ at the exterior and the interior of $K$. We see that (4.4) introduces the jump of $u_i$ on the upwind part $\partial K_-$ of $\partial K$. Using the jump evidently tries to take into account that the derivative of a discontinuous function contains Dirac masses at the point of discontinuity.

This scheme can be made somewhat more general. It was suggested to us by Raviart to use instead of (4.3),

$$(u', v) - \sum_K \left( \int_K (u_i u_j) \frac{\partial v_i}{\partial x_j} \, dx - \int_{\partial K} u \cdot n ((1 - \alpha) \, u_i^- + \alpha u_i^+) \, v_i \, d\sigma \right)$$
$$= \int_\Omega f_i v_i \, dx, \qquad \forall v \in H_h , \tag{4.5}$$

or equivalently

$$(u', v) + \sum_K \left( \int_K \frac{\partial}{\partial x_j} (u_i u_j) \, v_i \, dx + \alpha \int_{\partial K_-} u \cdot n [u_i] \, v_i \, d\sigma + \cdots \right.$$
$$\left. + (1 - \alpha) \int_{\partial k_+} u \cdot n [u_i] \, v_i \, d\sigma \right) = \int_\Omega f_i v_i \, dx, \qquad \forall v \in H_n .$$

For $\alpha = \frac{1}{2}$ we clearly get a "centered" discrete derivative. For $\alpha = 1$ we get back (4.3) and for $\alpha < \frac{1}{2}$ we have downwind derivatives which clearly lead to an unstable method. We now show that for $\alpha > \frac{1}{2}$ this scheme is dissipative. Indeed making $v = u$ in (4.6) it is a matter of tedious computation to get, for $f \equiv 0$,

$$\frac{1}{2}\frac{d}{dt}|u|_{L^2}^2 + \frac{(2\alpha - 1)}{2}\sum_S \left(\int_S ([u_1]^2 + [u_2]^2)u \cdot n \, d\sigma\right) = 0. \tag{4.7}$$

Here the sum is taken on all interfaces $S$ and $n$ is chosen such that $u \cdot n$ be positive. For $\alpha > \frac{1}{2}$ the second term is positive and we then lose energy with time. As $u \cdot n$ is continuous $[u_1]^2 + [u_2]^2$ reduces to $[u \cdot \tau]^2$. Thus dissipation is related to jumps of tangential velocity on interfaces.

## 5. Error Analysis of the Method

We shall not attempt here to present a complete analysis, which is anyway out of reach because of the nonlinearity of the problem. We therefore restrict ourselves to a linearized model. Then let

$$a = \{a_i\}, \qquad i = 1,..., N, \tag{5.1}$$

be a known solenoidal vector field such that $a \cdot n|_\Gamma = 0$. We consider a *model* steady-state problem. ($\sigma$ is a strictly positive constant)

$$\frac{\partial u_i}{\partial t} + \frac{\partial}{\partial x_j}(a_j u_i) + \sigma u_i + \frac{\partial p}{\partial x_i} = f, \tag{5.2}$$

$$\operatorname{div} u = 0, \tag{5.3}$$

$$u \cdot n|_\Gamma = 0, \qquad u_i(x, 0) = u_i^0(x) \text{ known}. \tag{5.4}$$

It is clear that such a problem can be readily approximated by the finite-element method of Section 4.

We suppose that the discrete velocities $u_h \in H_h$ are piecewise polynomial functions of degree $k$. In our numerical examples (Section 9), $k$ is equal to 1. From Lesaint [14] and Lesaint–Raviart [15] we deduce that we can get an error estimate on $|u - u_h|$, (in $(L^2(\Omega))^N$), which is $O(h^k)$ where $h$ is the mesh size. This can be extended to $O(h^{k+1/2})$ for special cases. This result is not optimal in the sense that one could expect $O(h^{k+1})$ for an error estimate in $L^2(\Omega)$ norm.

Lesaint [14] shows that the result can be made optimal if the elements are quadrilaterals such that any element has only two "lighted sides" (i.e., sides where $a \cdot n < 0$). For triangles, one should have that any element has one side parallel to the direction field $a$, which is a quite strong requirement. This analysis makes think that quadrilaterals would be more natural elements for this kind of approximation.

*Remark* 5.1. The error estimates of Lesaint [14] are derived when $\alpha = 1$. When we have $\alpha > \frac{1}{2}$, it is easy to check that the same results hold.

## 6. Time Discretization and Computational Aspects

### 6.1. *General Remarks*

In order to complete the description of the method, we must now discretize the time derivative and describe some computational features. To simplify the exposition, we shall denote in the sequel for $u, v, w \in H_h$.

$$b_h(u, v, w) = \sum_K \left\{ - \int_K u_i v_j \frac{\partial w_j}{\partial x_i} \, dx + \int_{\partial K} u \cdot n v_i^+ w_i \, d\sigma \right\}. \tag{6.1}$$

We now consider, to approximate (4.3), a predictor–corrector scheme with $O(\Delta t^2)$ accuracy. The computation proceeds as follows:

#### 6.1.1. *Predictor*: *Leap-Frog Scheme*

Let $u^n$ denote the value of the velocity at time $t = n\,\Delta t$. If $u^n$ and $u^{n-1}$ are known, we compute a first guess $u_0^{n+1}$ of $u^{n+1}$ by

$$\frac{1}{2\Delta t}(u_0^{n+1} - u^{n-1}, v) + b_h(u^n, u^n, v) = (f, v), \qquad \forall v \in H_h \tag{6.2}$$

#### 6.1.2. *Corrector*: *Gear's Scheme*

The predictor $u_0^{n+1}$ being know, we define $u_{k+1}^{n+1}$ from $u_k^{n+1}$ through

$$\frac{1}{\Delta t}\left(\frac{3}{2} u_{k+1}^{n+1} - 2u^n + \frac{1}{2} u^{n-1}, v\right) + b_h(u_k^{n+1}, u_k^{n+1}, v) = (f, v), \qquad \forall v \in H_h. \tag{6.3}$$

This iteration is stopped as soon as, $\epsilon$ being small,

$$| u_{k+1}^{n+1} - u_k^{n+1} | < \epsilon. \tag{6.4}$$

This is, of course, a fixed-point procedure $u_{k+1}^{n+1} = T(u_k^{n+1})$, and convergence will require the condition $\| T'(u^{n+1}) \| < 1$. For this particular case, this implies that a Courant–Friedrichs–Levy-type condition must be set on $\Delta t$, namely, in first approximation,

$$\frac{\sup_x | u(x) | \, \Delta t}{\inf_K \sigma(K)} < C_0, \tag{6.5}$$

where $\sigma(K)$ is the diameter of the largest inscribed circle for triangle (or element) $K$. The constant $C_0$ depends on the type of elements used and is rather hard to determine a priori. Of course, the smaller the $\Delta t$, the faster the convergence. In practice, this can be used to develop *an automatic time-step strategy*. For instance one way is that (6.4) should be verified for $k = 1$. Then $\Delta t$ is reduced whenever this fails or increased if (6.4) is systematically verified with $k = 0$.

The predictor–corrector scheme cannot be used for the first step. We used as a starting-up procedure, a Crank–Nicholson step.

$$\frac{1}{\Delta t}(u^1 - u^0, v) + \frac{1}{2} b_h(u^1, u^1, v) + \frac{1}{2} b_h(u^0, u^0, v) = (f, v), \qquad \forall v \in H_h . \quad (6.6)$$

This nonlinear equation is solved by the same kind of iterative procedure as in (6.3).

This time-discretization procedure is, of course, only one possible choice among others. It would also have been attractive to use an implicit Runge–Kutta scheme (cf. Crouzeix [6]). A conceptual advantage is that such scheme can be deduced from a time–space finite-element discretization. (cf. Lesaint–Raviart [15]), thus giving a similar treatment to both time and space derivatives.

From a computational point of view, it must be pointed out that computing $u_{k+1}^{n+1}$ in (6.3) or $u_0^{n+1}$ in (6.2) implies the resolution of a discrete Dirichlet problem for the stream function $\psi^{n+1}$. Indeed our space $H_h$ has been defined by taping the curl of a piecewise quadratic conforming approximation $W_{0h}^k$ for $\psi$. We thus have

$$(u^{n+1}, v) = (\text{rot } \psi^{n+1}, \text{rot } \phi) = -\langle \Delta_h \psi^{n+1}, \phi \rangle, \qquad \forall \phi \in W_{0h}^k . \quad (6.7)$$

It is possible to factorize the discrete Laplacian matrix once and for all using Cholevsky's algorithm. A more precise discussion of this point and details on the computation of nonlinear terms may be found in Thomasset [19]. In particular, this references treat the case of domains with holes where a slight modification of Cholevsky's algorithm can be used.

### 6.2. *Numerical Results, Euler's Equations*

We tested the above scheme on the two problems described below in order to bring into evidence the effects of artificial damping.

#### 6.2.1. *Problem* I: *Evolution of a "Gaussian Vortex"*

Let $\Omega$ be the unit circle ($r^2 = x^2 + y^2 < 1$) and initial conditions be given by

$$\psi(x_1, x_2, 0) = \exp(-100r^2) - \exp(-100). \quad (6.8)$$

The initial streamlines are shown on Fig. 1. We require $\psi \equiv 0$ at the boundary and let the system evolve. It is an easy matter to check that the exact solution should remain constant with respect to time. The number of triangles is 400 (mesh size 1/10) and the time step $\Delta t$ is $10^{-3}$. Computations were performed with various values of $\alpha$. Figure 2 shows the streamlines at time $t = 0.082$ for $\alpha = 1$ and Fig. 3 shows the similar result with $\alpha = 0.51$. We see that counter vortices are developing due to artificial viscosity.

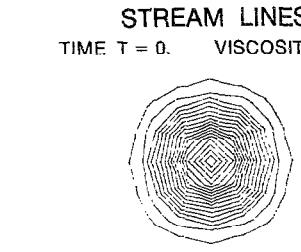


INITIAL STATE
FIGURE 1

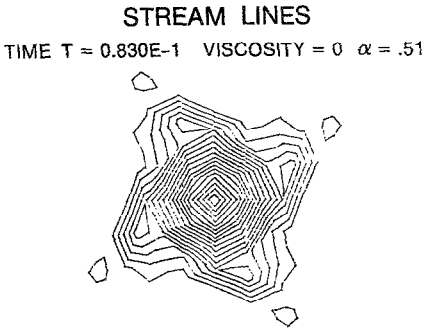


FIGURE 2

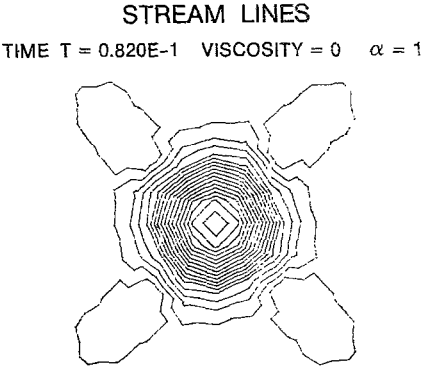


FIGURE 3

We also plot on Fig. 4 the variation of the kinetic energy,

$$E(t) = \int_{\Omega} |\, \mathbf{u}_h(t)|^2 \, dx, \tag{6.9}$$

versus time $t$. As expected, the damping is by far more important for $\alpha = 1$ than for $\alpha$ near 0.5. Numerical experience shows that $\alpha = 0.5$ leads to instability.

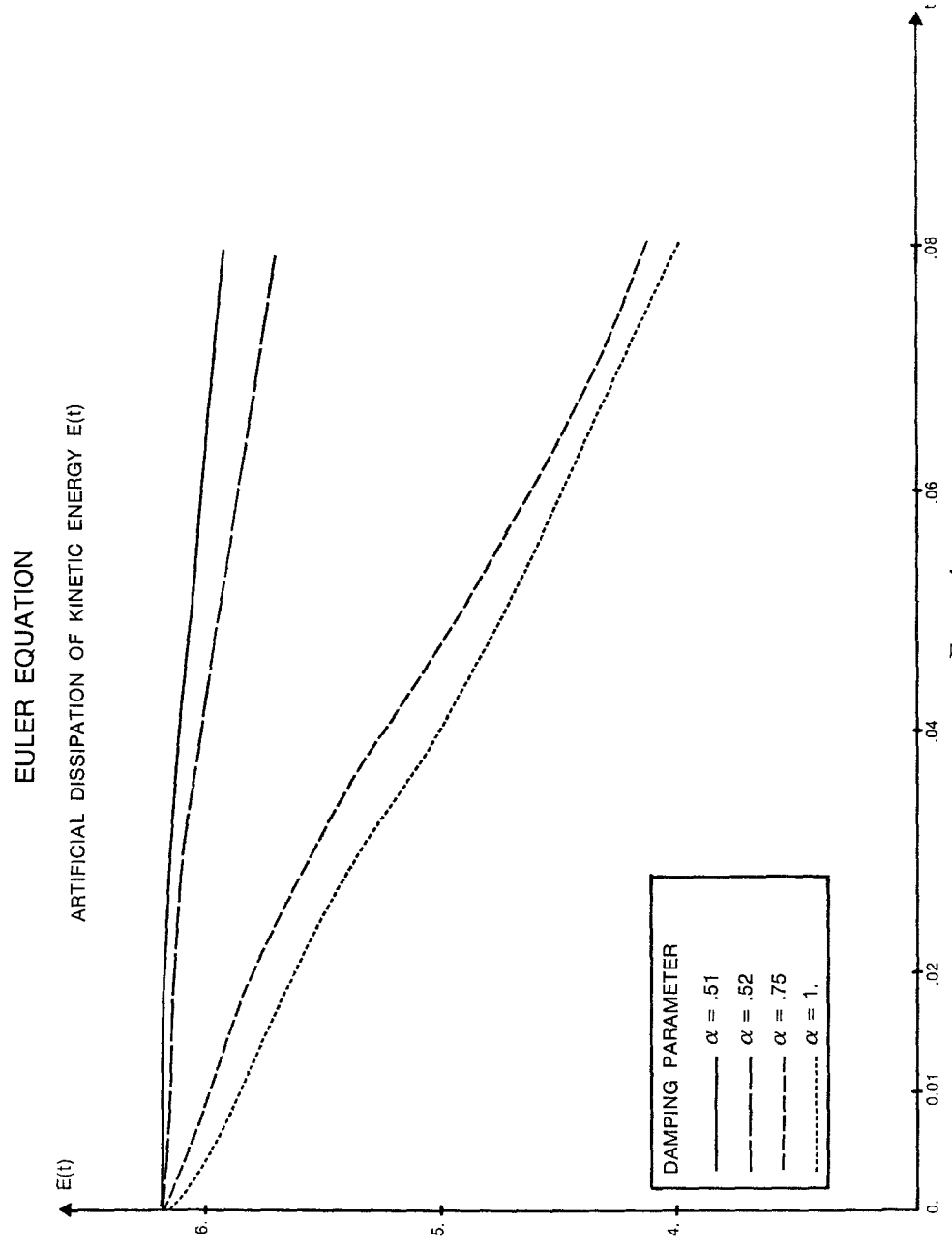
EULER EQUATION
ARTIFICIAL DISSIPATION OF KINETIC ENERGY E(t)
E(t)
6.
5.
4.
0.
0.01
.02
.04
.06
.08
t
DAMPING PARAMETER
α = .51
α = .52
α = .75
α = 1.

FIGURE 4

6.2.2. *Problem* II: *Flow past a Corner*

The corner domain is shown in Fig. 5. In the shaded region, we assume a body force

$$\mathbf{f}(x_1, x_2, t) = \begin{cases} \begin{pmatrix} 0 \\ 1 \end{pmatrix}, & \text{if } x_1 > 1 \text{ and } t \leqslant 4\Delta t, \\ \begin{pmatrix} 0 \\ 0 \end{pmatrix}, & \text{otherwise.} \end{cases} \tag{6.10}$$

The value of $\Delta t$ was $10^{-2}$ and 168 triangles were used. The initial state is shown in Fig. 6. The fluid is at rest behind the corner. Figure 7 presents the stream lines at time $t = 6.8$ for $\alpha = 1$. We see that a counter vertex has grown in the upper left region past the corner. showing a numerical viscosity effect. The solution is steadily decreasing, remaining self-similar, after this time.

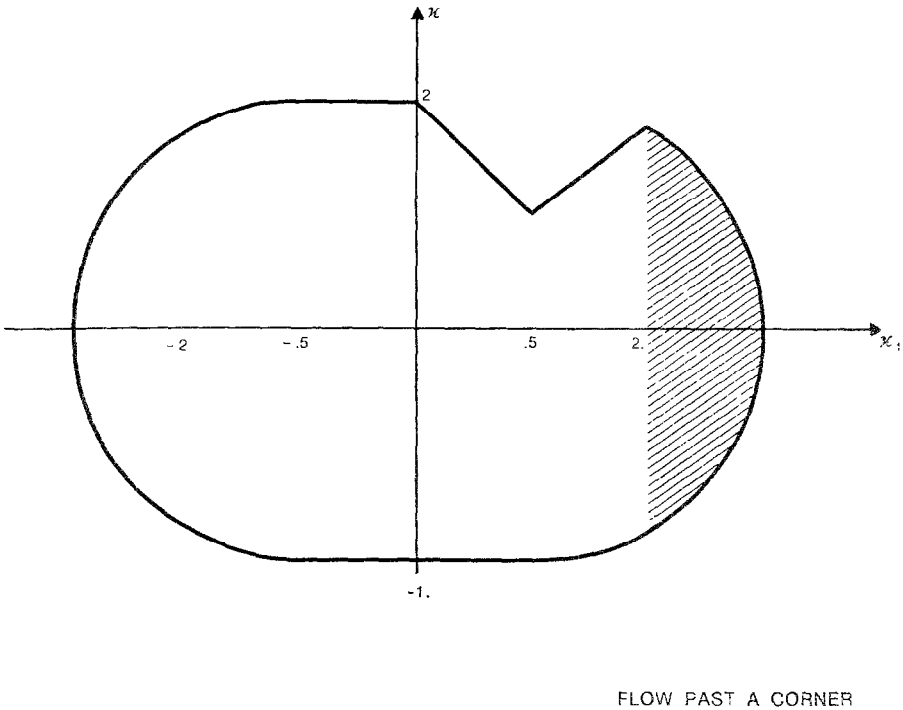


FIGURE 5

In conclusion we may state that the present method allows stable computations of inviscid flow. Numerical viscosity implies that it will be convenient to compute

smooth solutions. However, for highly irregular solutions that could be expected with some initial conditions it is probable that damping will be much too large to get a very good approximation.

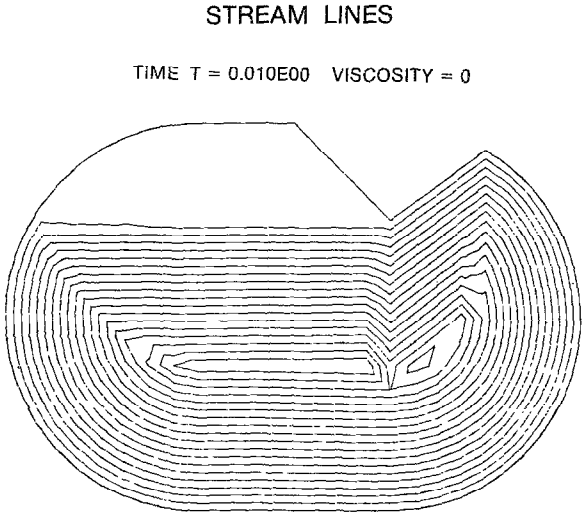


FIGURE 6

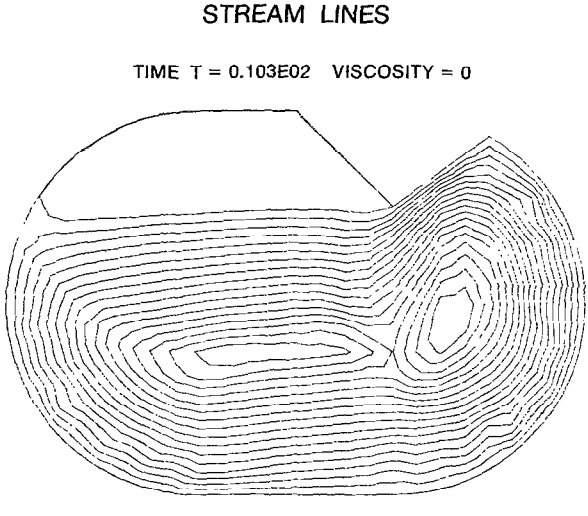


FIGURE 7

## 7. Steady Creeping Flow through Mixed Methods

In order to justify the treatment of viscous terms we shall use in the full Navier–Stokes equations, we consider first the classical steady-state Stokes problem which describes a viscous flow at very small Reynolds number. Nonlinear convective terms may then be neglected and we have to solve a linear system.

$$-\Delta u + \operatorname{grad} p = f, \tag{7.1}$$

$$\operatorname{div} u = 0, \tag{7.2}$$

$$u|_\Gamma = 0. \tag{7.3}$$

Equations (7.1)–(7.2) must be satisfied in a domain $\Omega \subset \mathbb{R}^N$ ($N = 2$ or 3). We suppose, to simplify the exposition, that $\Omega$ is bounded, simply connected, and that $\Gamma = \partial\Omega$ is smooth enough (for instance, Lipschitzian). When $N = 2$, it is well known that this problem is equivalent to a biharmonic problem. Let $\psi$ be the stream function such that $u = \operatorname{curl} \psi$ ($= \nabla \times \psi$). Then solving (7.1)–(7.3) is equivalent to solving

$$\Delta^2 \psi = \operatorname{curl} f, \tag{7.4}$$

$$\psi|_\Gamma = \frac{\partial \psi}{\partial n}\Big|_\Gamma = 0. \tag{7.5}$$

This remark will be important, for we shall rely, to approximate (7.1)–(7.3) on classical methods for (7.4)–(7.5). However, the final result will not be restricted to the two-dimensional case. Mixed methods are related to saddle-point variational principles.

To avoid long preliminaries, we shall introduce them as a mere reduction of a second-order problem to a first-order system.

In this section we shall analyze a mixed method that will be based on the following identity for the vector Laplacian operator

$$-\Delta u = \operatorname{curl} \operatorname{curl} u - \operatorname{grad} \operatorname{div} u. \tag{7.6}$$

Using (7.2) and (7.6) and setting $\omega = \operatorname{curl} u$, we can then write (2.1)–(2.3) as a system;

$$\operatorname{curl} \omega + \operatorname{grad} p = f, \tag{7.7}$$

$$\omega = \operatorname{curl} u, \tag{7.8}$$

$$\operatorname{div} u = 0, \tag{7.9}$$

$$u|_\Gamma = 0. \tag{7.10}$$

Using the function space $V$ defined in Section 2, we now write these equations in weak form, multiplying (7.7) by $v \in H$ and (7.8) by $\phi \in H^1(\Omega)$. We then have,

$$(\operatorname{curl} \omega, v) - (f, v) = 0, \qquad \forall v \in H, \tag{7.11}$$

$$\begin{aligned}(\omega, \phi) = (\operatorname{curl} u, \phi) &= (u, \operatorname{curl} \phi) + \int_\Gamma u \cdot \tau \phi \, d\sigma \\ &= (u, \operatorname{curl} \phi), \qquad \forall \phi \in H^1(\Omega).\end{aligned} \tag{7.12}$$

Let us recall that $u \in H$ means $\operatorname{div} u = 0$ and $u \cdot n = 0$. The no-slip boundary condition is thus included in a weak form in (7.12). It can be shown that the unique solution to (7.1)–(7.3) is also a solution to (7.11)–(7.12). However, it must be pointed out that (7.11)–(7.12) is a weaker formulation of the problem as it no longer requires $u_i \in H_0^1(\Omega)$.

If we now restrict ourselves to the bi-dimensional case, we can write $v \in H$ as $v = \operatorname{curl} \phi_0$, $\phi_0 \in H_0^1(\Omega)$. Then we have

$$(\operatorname{curl} \omega, \operatorname{curl} \phi_0) = (f, \operatorname{curl} \phi_0), \qquad \forall \phi_0 \in H_0^1(\Omega), \tag{7.13}$$

$$(\omega, \phi) = (\operatorname{curl} \psi, \operatorname{curl} \phi), \qquad \forall \phi \in H^1(\Omega), \tag{7.14}$$

or more classically, neglecting boundary conditions,

$$-\Delta \psi = \omega, \tag{7.15}$$

$$\Delta \omega = \operatorname{curl} f \tag{7.16}$$

with appropriate boundary conditions.

The numerical approximation of (7.13)–(7.14) has been studied in Ciarlet–Raviart [5] and algorithms for solution are given in Ciarlet–Glowinski [4] and Glowinski–Pironneau [11]. In the two-dimensional case, the discretization of [5] is strictly equivalent to the one we have used and error analysis results may be obtained directly from their results.

The discretization proceeds as follows. We consider the space $W_h^k$ of Section 3 of conforming elements approximating $H^1(\Omega)$. We then have a space of discrete functions which are piecewise polynomials of degree $k$ on each element and which are continuous on element interfaces. $W_h^k$ is the space of discrete vorticities $\omega_h$.

Let $W_{0h}^k$ be the subspace of $W_h^k$ such that $\psi_h \in W_{0h}^k$ iff $\psi_h|_\Gamma = 0$.

Then Section 3, we define $H_h$ by taking

$$H_h = \{v_h \mid v_h = \operatorname{curl} \psi_h, \psi_h \in W_{0h}^k\}. \tag{7.17}$$

The discrete problems are then

$$(\operatorname{curl} \omega_h, v_h) - (f, v_h) = 0, \qquad \forall v_h \in H_h, \tag{7.18}$$

$$(\omega_h, \phi_h) = (u_h, \operatorname{curl} \phi_h), \qquad \forall \phi_h \in W_h^k, \tag{7.19}$$

or equivalently,

$$(\operatorname{curl} \omega_h, \operatorname{curl} \gamma_h) = (f, \operatorname{curl} \gamma_h), \qquad \forall \gamma_h \in W_{0h}^k, \tag{7.20}$$

$$(\omega_h, \phi_h) = (\operatorname{curl} \psi_h, \operatorname{curl} \phi_h), \qquad \forall \phi_h \in W_h^k, \tag{7.21}$$

$$w_h \in W_h^k, \qquad \psi_h \in W_{0h}^k. \tag{7.22}$$

It must be noted that, whenever one has built a discrete space $H_h \subset H$ in a consistent

The error analysis of Ciarlet and Raviart shows that the precision of this scheme is $O(h^{k-1})$ (where $h$ is the mesh size). This results holds for $| u - u_h |_{L^2(\Omega)}$ and $| \omega - \omega_h |_{L^2(\Omega)}$.

The expected estimate would be $O(h^k)$. There is a loss of precision with respect to the degree of polynomials used. If one uses as in the present numerical computations of Section 6, piecewise quadratic polynomials, the expected precision will be $O(h)$ instead of $O(h^2)$. Numerical evidence shows that problems are restricted to values of $\omega$ along the boundaries and that values of $\psi$, $u$, and $\omega$ away from walls are better than the predictions of error analysis (cf. Bourgat [1]).

*Remark* 7.1. We have considered up to now the case of inhomogeneous boundary conditions. It is a simple task to introduce nonhomogeneous tangential boundary conditions. Setting, instead of (7.21),

$$(\omega_h , \phi_h) = (u_h , \operatorname{curl} \phi_h) - \int_\Gamma g\phi_h \, d\sigma \tag{7.23}$$

implies the solution has to satisfy

$$u_h |_\Gamma = g \tag{7.24}$$

in a weak sense. It is also possible to impose boundary conditions on $\omega$. This is, of course, seldom of any practical use.

*Remark* 7.2. It appears that for $N = 2$, the method is just a rewriting of a standard mixed method for the biharmonic problem. It is also possible to adapt such mixed methods as the Hermann–Johnson scheme (cf. Johnson [12] and Brezzi–Raviart [2]) to the solution of Stokes problem. Such an approach has been suggested in Fortin [9]. The basis of the development is to write (7.1) as

$$-\sum_j \frac{\partial p_{ij}}{\partial x_j} + \frac{\partial p}{\partial x_i} = f_i , \tag{7.25}$$

$$p_{ij} = \frac{\partial u_i}{\partial x_j} , \tag{7.26}$$

and then to approximate $p_{ij}$ in a proper way. A theoretical advantage is that the expected precision is now optimal with respect to the degree of polynomials used in the finite-element approximation. We do not develop further this point as we have no numerical results, up to date; this method is heavier to handle than the previous one.

*Remark* 7.3. From a physical point of view, it would be natural to use the stress tensor $\sigma_{ij}$ instead of $p_{ij}$ in (7.25)–(7.26). Some problems arise however in finite-elements approximations, with respect to the symmetry of $\sigma_{ij}$. This can be probably be overcome and the interest of such approximations would be to handle directly boundary conditions on $\sigma_{ij}$, which are quite often encountered.

## 8. A Mixed Method for the Navier–Stokes Equations

We are now able to state a complete scheme for viscous incompressible flow that uses solenoidal elements for the velocity vector field, upwind derivatives for nonlinear terms, and that allows a discontinuity of the tangential component of velocity on elements interfaces. This scheme uses the discretization of Euler's equations of Section 4. In semidiscrete form, we may write

$$(u_h', v_h) + \nu(\text{curl } w_h, v_h) - \sum_k \left\{ \int_K (u_{ih}, u_{jh}) \frac{\partial v_i}{\partial x_j} \right) + \int_{\partial K} u \cdot n(u_i^\alpha v_i)\, d\sigma \Big\}$$
$$= (f_i, v_i), \qquad \forall v_h \in H_h, \quad u_h \in H_h, \tag{8.1}$$
$$u_i^\alpha = \alpha u_i^+ + (1 - \alpha) u_i^-$$
$$(\omega_h, \phi_h) = (u_h, \text{curl } \phi_h), \qquad \forall \phi_h \in W_h. \tag{8.2}$$

It must be noted that $u_h \in H_h$ implies $u_h \cdot n|_\Gamma = 0$. Condition (8.2) implies $u_h \cdot \tau|_\Gamma = 0$ in a weak form. Non-homogenous boundary conditions can easily be implemented.

The time discretization we used in our numerical computations was the same as the one discussed in Section 6 for inviscid flow. We thus used an implicit scheme. Corrector iterations had now to be done on both (8.1) and (8.2). We point out that any time discretization *must be implicit* in $\omega_h$ if the no-slip boundary condition is to be satisfied. Following Glowinski–Pironneau [11] it should be possible to devise much better solution methods to replace the rude corrector iteration. This is the object of current work and is related to the setting of an efficient steady-state solver. In present computations, steady states have been obtained through a time-dependent problem. Following Remark 7.2 a similar scheme has been proposed in Fortin [9], using $p_{ij} = \partial u_i/\partial x_j$ as a "dual" variable.

*Remark* 8.1. An important feature of this kind of scheme is that viscosity or dissipation appears as a separate mechanism which is simulated through the use of vorticity or another auxiliary field. This makes very easy the computation of non-Newtonian flows as for instance, only the law relating $\omega_h$ to $u$ has to be changed in (8.2). Similarly it would be quite simple to introduce an extra viscous term modeling turbulent dissipation.

## 9. Navier–Stokes Equations: Numerical Results

### 9.1. *Square Wall-Driven Cavity*

$\Omega$ is the unit square: ]0, 1[ × ]0, 1[ (Fig. 8). We assume the following *boundary* conditions:

$$\mathbf{u}(x_1, x_2) = \begin{pmatrix} 0 \\ 0 \end{pmatrix}, \qquad \text{if} \quad x_2 < 1,$$
$$\mathbf{u}(x_1, x_2) = \begin{pmatrix} 1 \\ 0 \end{pmatrix}, \qquad \text{if} \quad x_2 = 1.$$

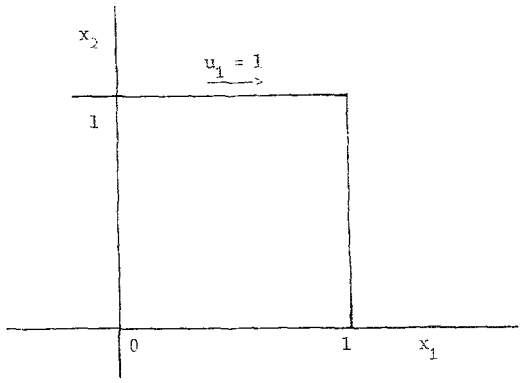


FIGURE 8

Thus, the nominal Reynolds number is $\mathrm{Re} = 1/\nu$. We used regular meshes, of which characteristics are given in Table I. (It is divided into $N^2$ equal squares, each square being divided into 2 triangles.)

TABLE I

| | $h = 1/8$ | $h = 1/12$ | |
|---|---|---|---|
| Number of triangles | 128 | 288 | |
| Number of vertices | 81 | 169 | |
| Number of mind side nodes | 208 | 456 | |
| Number of unknowns for Laplace's equation | 225 | 529 | (Number of unknown values of $\psi$) |
| Bandwidth for Laplace's equation | 37 | 53 | |
| Bandwidth for $\omega$ equation | 42 | 58 | |
| Average computer time per time step | 1.9 sec (IBM-370-168) | 2 min, 10 sec (CII-IRIS 80) | |
| Total number of unknowns | 514 | 1144 | |

*Note.* The use of a regular mesh does not take full advantage of the possibilities of the finite-element method; however, this choice allows

(1) an easy comparison with finite-difference methods;

(2) a study of convergence when the mesh size $h = 1/N$ is decreased.

We tried several values of viscosity: $\nu = 10^{-2}, 10^{-3}, 10^{-4}$; we sum in Table II the results of computations.

TABLE II

| | $\nu$ | $10^{-2}$ | $10^{-3}$ | $10^{-4}$ |
|---|---|---|---|---|
| $h = 1/8$ | $\Delta t$ | 0.3[b] | 0.03 | 0.03 |
| | $\alpha$ | 1. | 1. | 1. |
| Initial values | | Fluid at rest | Solution for $\nu = 10^{-2}$ | Solution for $\nu = 10^{-3}$ |
| Number of time cycles | | 500 | 650 | 1622 |
| $h = 1/12$ | $\Delta t$ | — | 0.02[a] | 0.02 |
| | $\alpha$ | | 1. | 1. |
| Initial values tim | | — | Moving fluid[b] | Solution for $\nu = 10^{-3}$ |
| Number of time cycles | | — | 850 | 2000 |

[a] Maximum $\Delta t$ allowed.
[b] $\psi(x_1, x_2; 0) = -2.7x_1(1 - x_1)x_2^2(1 - x_2)$.

We plot in Figs. 9–12 the velocity profile along the midline $x_1 = \frac{1}{2}$. (The first component $u_1$ is well defined along this line because it is a boundary line between triangles in our mesh, $u_1$ being the normal velocity.) We compare the results with some finite-difference schemes:

—for $\nu = 10^{-2}$ with Burggraf's results [3];

—for $\nu = 10^{-3}$ with Fortin *et al.* [10];

—for $\nu = 10^{-4}$ we do not know of any computation for the same problem; we give as an indication the limit given by Burggraf [3] when $\nu \to 0$. On Fig. 12 we show the influence of $\alpha$. The streamlines are shown on Figs. 13 ($\nu = 10^{-2}$, $h = 1/8$), Fig. 14 ($\nu = 10^{-3}$, $h = 1/12$), and Fig. 15 ($\nu = 10^{-4}$, $h = 1/12$), and the vorticity lines on Figs. 16 ($\nu = 10^{-2}$, $h = 1/8$), Fig. 17 ($\nu = 10^{-3}$, $h = 1/12$), and Fig. 18 ($\nu = 10^{-4}$, $h = 1/12$).

*Remarks.* (1) The dotted lines in Figs. 14 and 15 stand for the line $\psi = 0$ and show the existence of counter vortices in the corners; such vortices are also present in Fig. 13 ($\nu = 10^{-2}$) although the line $\psi = 0$ is not plotted.

(2) The process was stopped when the difference between the degrees of freedom of $\psi$ at times $n\,\Delta t$ and $(m + 1)\,\Delta t$ was less than $10^{-5}$.

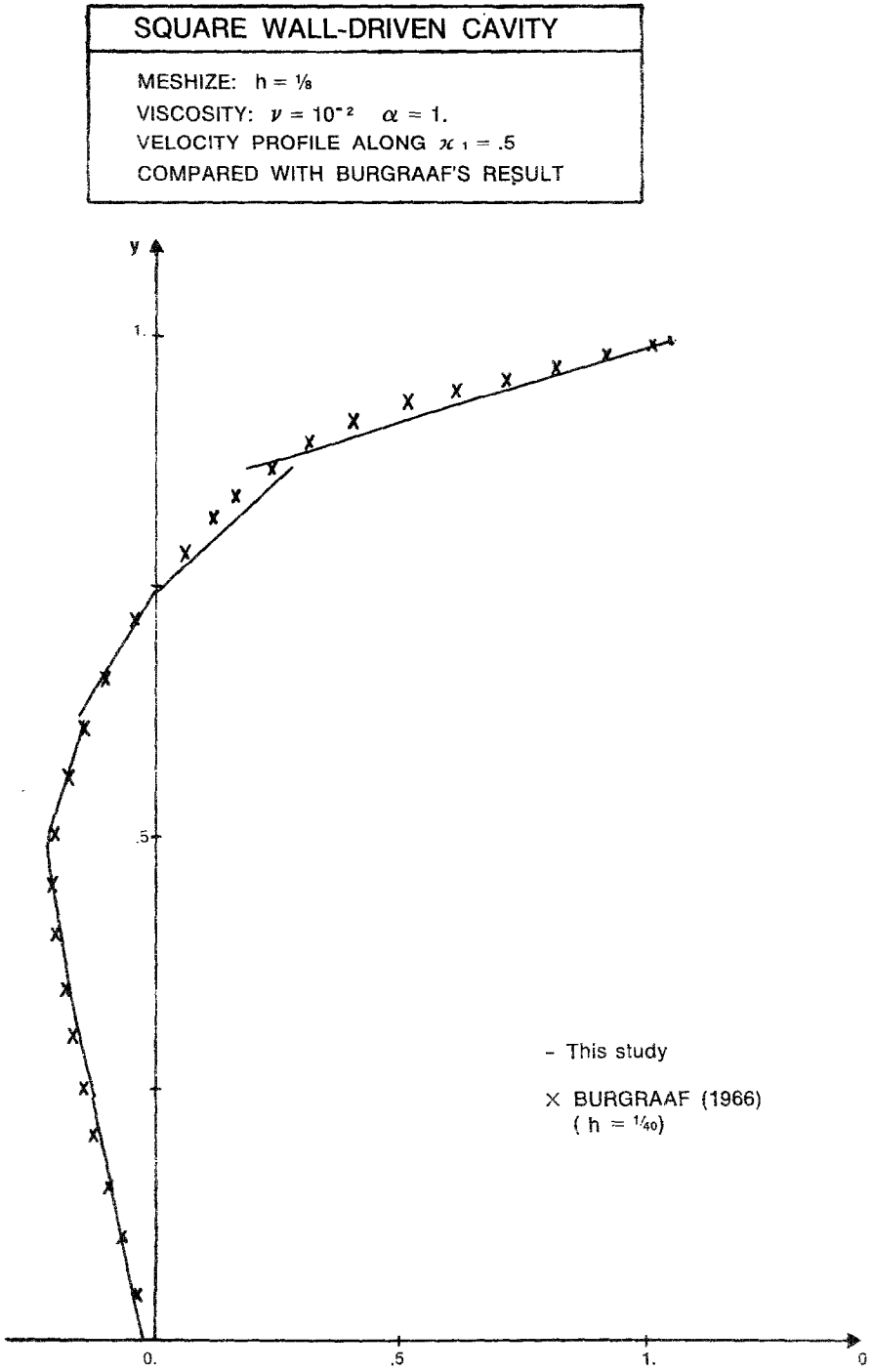
SQUARE WALL-DRIVEN CAVITY
MESHIZE: h = 1/8
VISCOSITY: ν = 10⁻²  α = 1.
VELOCITY PROFILE ALONG x₁ = .5
COMPARED WITH BURGRAAF'S RESULT
y
1.
.5
0.
.5
1.
0
- This study
× BURGRAAF (1966)
( h = 1/40)

FIGURE 9

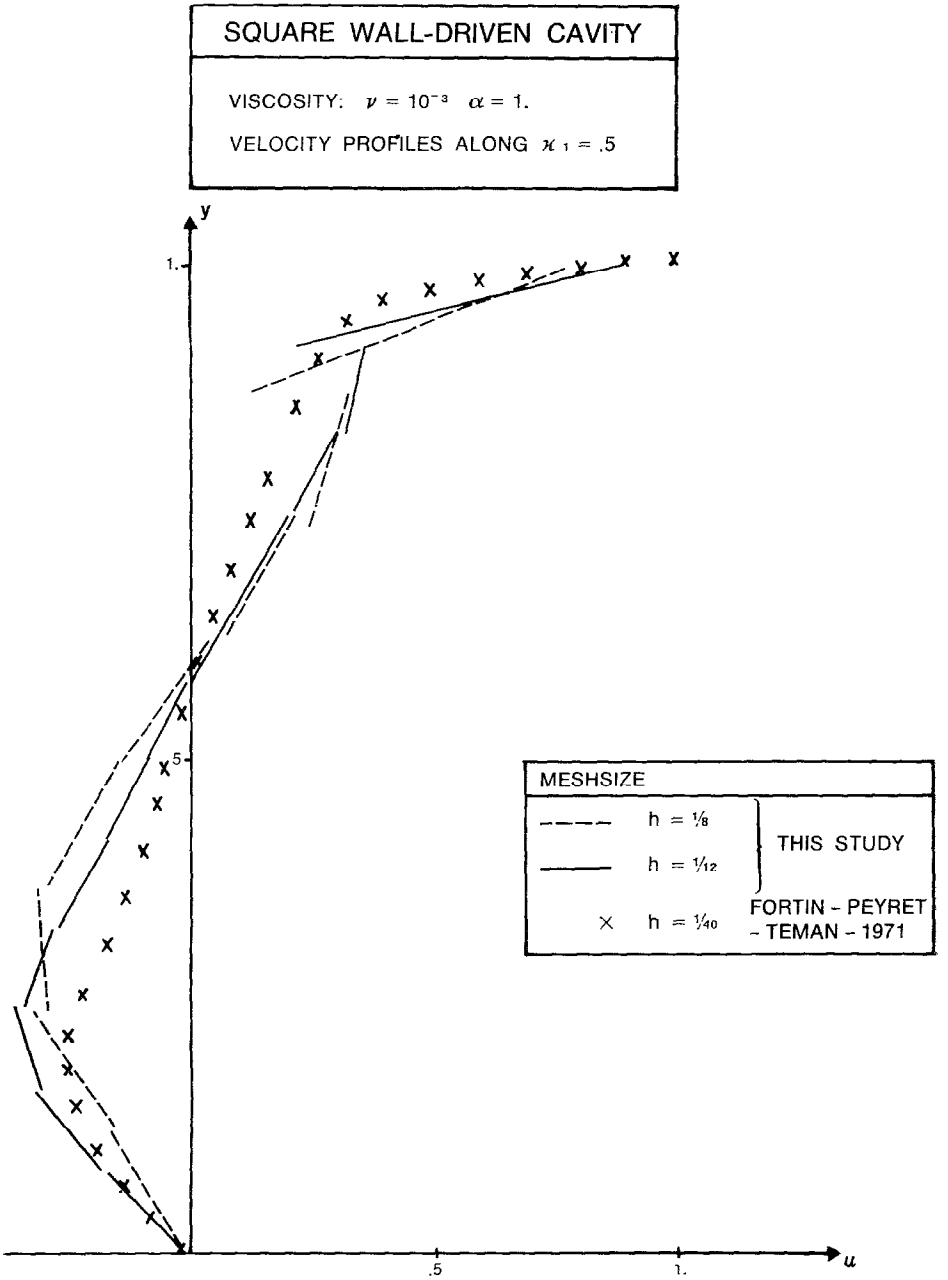
SQUARE WALL-DRIVEN CAVITY
VISCOSITY: $\nu = 10^{-3}$ $\alpha = 1.$
VELOCITY PROFILES ALONG $x_1 = .5$
y
1.
.5
.5
1.
u
MESHSIZE
h = 1/8
h = 1/12
THIS STUDY
h = 1/40
FORTIN - PEYRET - TEMAN - 1971

FIGURE 10

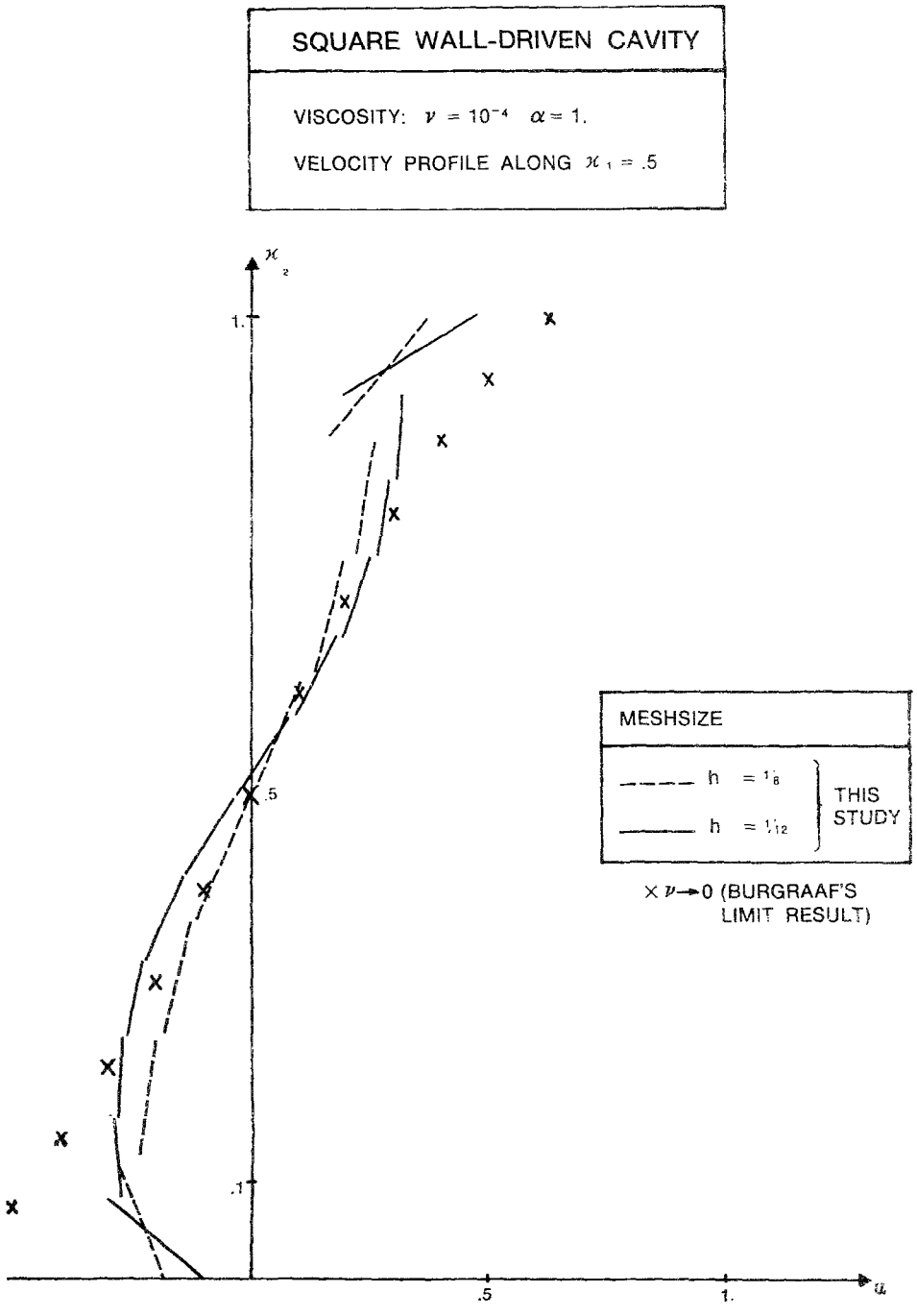
SQUARE WALL-DRIVEN CAVITY
VISCOSITY: $\nu = 10^{-4}$ $\alpha = 1.$
VELOCITY PROFILE ALONG $x_1 = .5$
$x_2$
1.
.5
.1
.5
1.
$u$
MESHSIZE
h = 1/8
h = 1/12
THIS STUDY
× $\nu \to 0$ (BURGRAAF'S LIMIT RESULT)

FIGURE 11

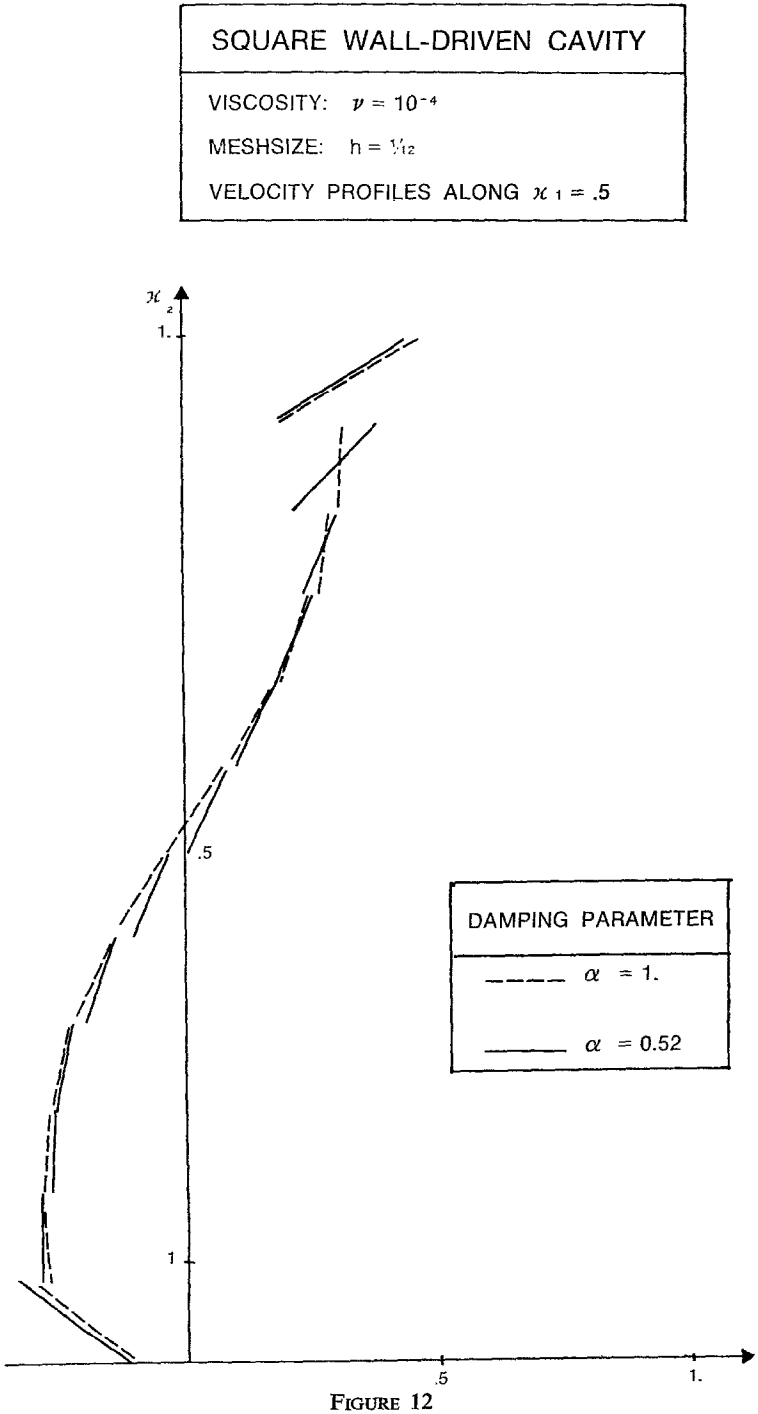
SQUARE WALL-DRIVEN CAVITY
VISCOSITY: $\nu = 10^{-4}$
MESHSIZE: h = 1/12
VELOCITY PROFILES ALONG $x_1 = .5$
$x_2$
1.
.5
1
.5
1.
DAMPING PARAMETER
$\alpha = 1.$
$\alpha = 0.52$

FIGURE 12

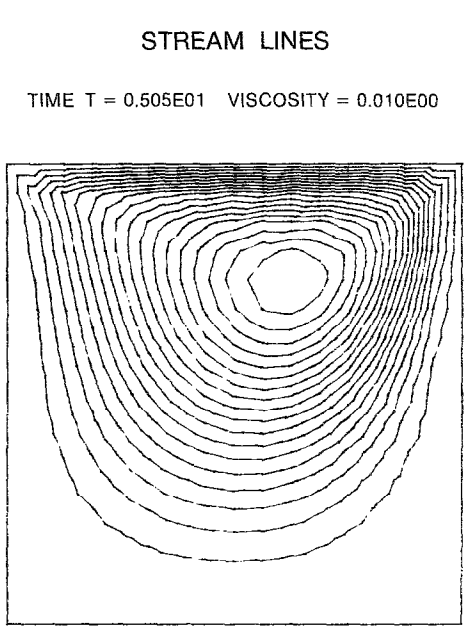


FIGURE 13

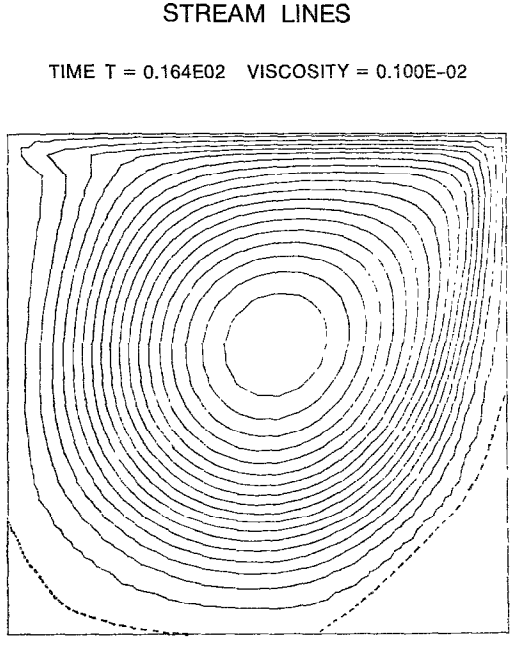


FIGURE 14

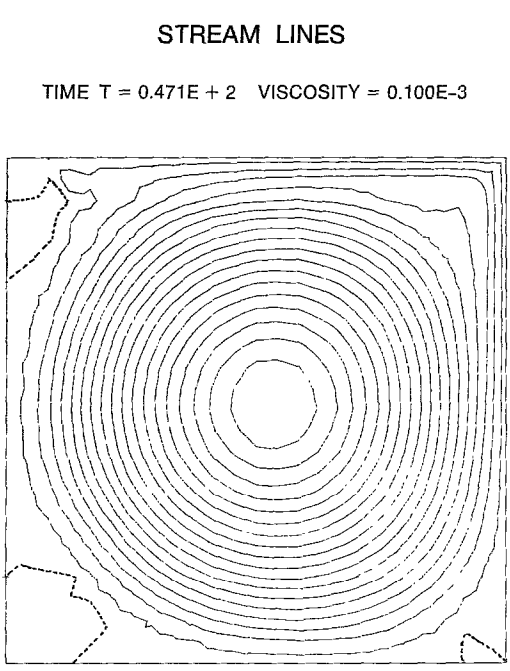


FIGURE 15

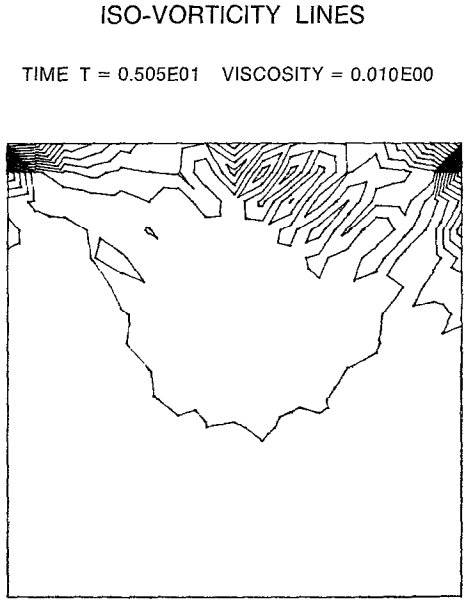


FIGURE 16

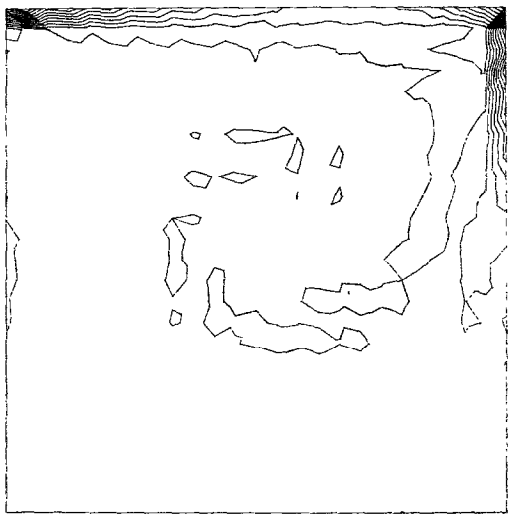


FIGURE 17

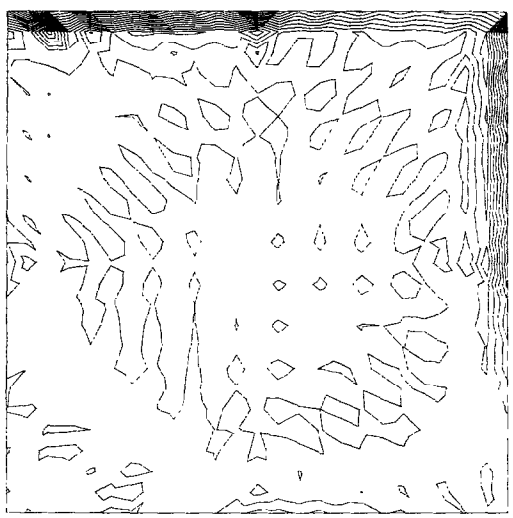


FIGURE 18

From these experiments a few conclusions may be drawn. First, the method proposed permits a fairly accurate computation at large Reynolds number with a relatively crude mesh size. The behavior for $\mathrm{Re} \to \infty$ can be expected to be correct if mesh is refined. The main problem is to devise an efficient way of computing steady-state solutions without going to an unsteady procedure. This is the object of current work and many possibilities are open.

### 9.2. *Flow past a Cylinder*

An obstacle $C_1$ (a cylinder of unit diameter) is placed in a fluid with uniform velocity at infinity. This problem is treated as being two dimensional. We assume that the influence of $C_1$ is negligible at points on a circle $C_2$, with same center and diameter 10.

We take as $\Omega$ the annular region between $C_1$ and $C_2$. On $C_2$ we have the boundary conditions

$$\begin{aligned} \mathbf{u} &= \mathbf{u}_\infty = \begin{pmatrix} 1 \\ 0 \end{pmatrix}, \\ \psi(x_1, x_2) &= x_2 . \end{aligned} \tag{9.1}$$

On the obstacle $C_1$, we just have

$$\psi \equiv \psi(C_1) = \text{unknown constant.}$$

Thus, the value of $\psi$ on $C_1$ is an unknown of the problem, to which corresponds to Eq. (9.1) (see Thomasset). As an initial value we took the irrotational solution, such that

$$\begin{aligned} -\Delta\psi &= 0, \qquad \text{in } \Omega, \\ \psi\,|_{C_1} &= \text{constant}, \\ \psi(x_1, x_2)\,|_{C_2} &= x_2 . \end{aligned}$$

TABLE 3

| | |
|---|---|
| Number of triangles | 144 |
| Number of vertices | 84 |
| Number of midside nodes | 228 |
| Number of unknown values of $\psi$ | 265 |
| Number of degrees of freedom of $\omega$ | 312 |
| Total number of equations | 577 |
| Bandwidth for $\psi$ equation | 69 |
| Bandwith for $\omega$ equation | 72 |
| Average CPU time for one time cycle | 40 sec (IBM 370–168)[a] |
| Time step: $\Delta t = 0.1$, $\alpha = 0.55$; $\nu = 0.02$. | |

[a] about 40 corrector iterations were performed at each time step.

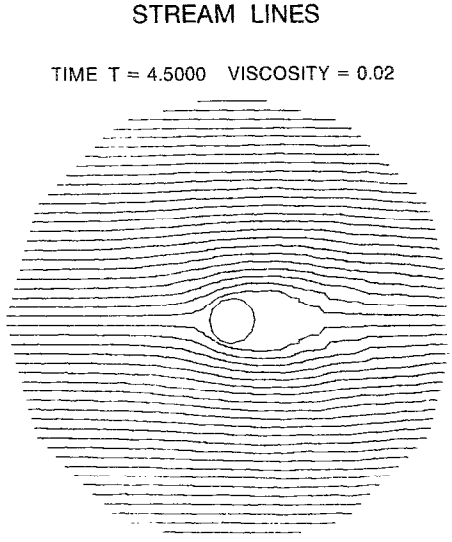


STEADY SYMMETRIC SOLUTION

FIGURE 19

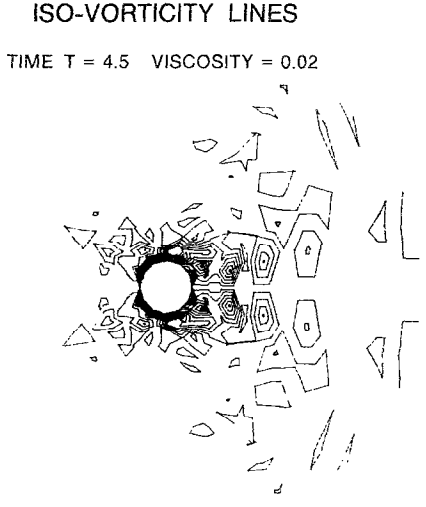


STEADY SYMMETRIC SOLUTION

FIGURE 20

We used a nonregular mesh, whose parameters are listed in Table III. We first obtained a stationary symmetric solution (Fig. 19: streamlines[1]; Fig. 20 vorticity lines). In order to break the symmetry, we perturbed this solution, multiplying by a factor of

[1] the counter vortices are not plotted, but do exist.

10 the value of $\psi$ at a point in the wake. After about 10 time cycles we obtain a Von Karman alley of eddies (Fig. 21).

The vortices in the Von Karman alley are seen to be very rapidly damped; this should be considered as an undesired influence of the downstream boundary $C_2$;

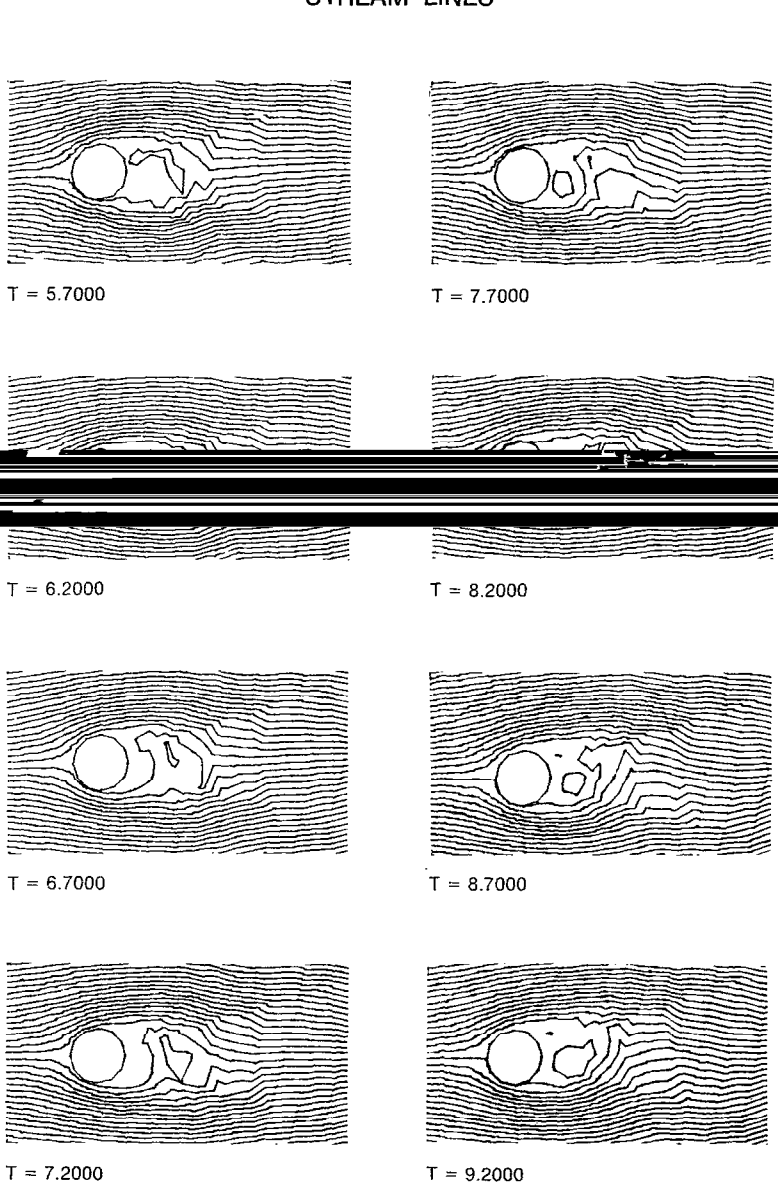


FIGURE 21

we can see also (Fig. 21) that the influence of the obstacle cannot be considered negligible at downstream points on $C_2$. This suggests than the computation should be done again with a downstream boundary $C_2$ at a greater distance from the obstacle ($C_2$ with other boundary conditions on $\psi$); this will be reported in a subsequent paper.

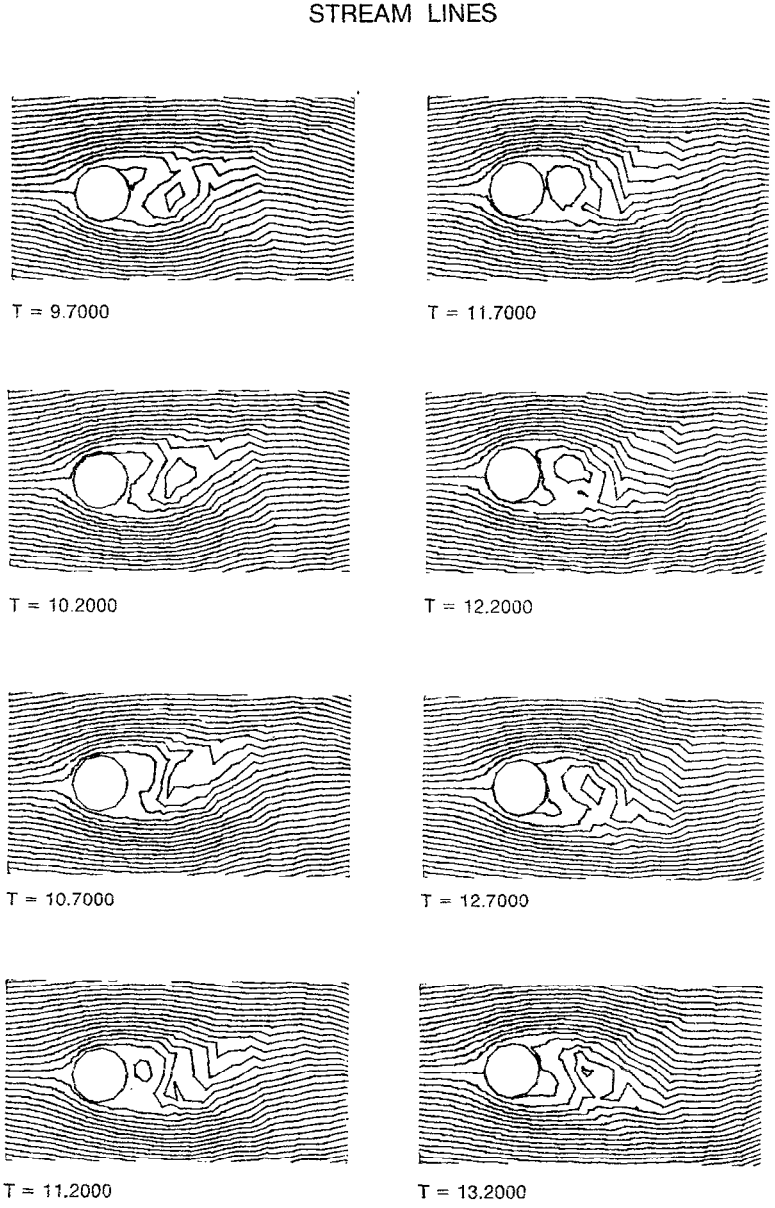


FIGURE 21 *(continued)*

## 10. Comments and Conclusion

At each time cycle we solved separately Eqs. (8.1) ($\psi$ equation) and (8.2) ($\omega$ equation) by a Cholevsky's algorithm for band-structured matrices (subroutine MCHB from IBM Scientific Subroutine Package). This requires the storage of two large matrices in factorized form; for instance, for the flow past a circle we had to store respectively 16,065 and 20,148 words.

Furthermore, the corrector iterations impose a stability condition on $\Delta t$. As expected we found this condition more and more straining as the mesh size is decreased. For a flow around an airfail with 60 triangle sides on the airfail and 1080 triangles we had to take $\Delta t = 10^{-5}$, which is too small to reasonably allow computations of practical interest. We are now testing some other solving procedures to make the overall process more efficient. We want to emphasize that the presented results are tests problems selected to test the accuracy of a discretization procedure. We are fully aware that much work remains to do in order to improve the efficiency in computation. The method studied implies nonstandard problems to be solved and it is clear that we may expect considerable improvements in the future. We are confident that finite-element methods of the type we have described will permit computations of viscous flows for fairly large Reynolds number with improved accurracy, all other things being equal. The authors want to thank MM. Perrier, Periaux, Poirier, and Mantel of "Les Avions Marcel Dassault–Breguet Aviation" for their help in programming facilities and computer time.

## References

1. J. F. Bourgat, Numerical applications of a dual iterative method for solving a finite element approximation of the biharmonic equation, Rapport 76-156, IRIA-LABORIA, 78150 Le Chesnay, France.
2. F. Brezzi and P. A. Raviart, Mixed finite element methods for fourth order elliptic equations (to appear), Rapport No. 9 École Polytechnique, Centre de Mathématiques Appliquées, Palaiseau, France.
3. O. R. Burgraf, Analytical and numerical studies of the structure of steady separated flows, *J. Fluid Mech.* **24** (1966), 113–151.
4. P. G. Ciarlet and R. Glowinski, Dual iterative techniques for solving a finite element approximation of the biharmonic equation, *Comput. Methods Appl. Math. Engrg.* **5** (1975), 277–295.
5. P. G. Ciarlet and P. A. Raviart, A mixed finite element method for the biharmonic equation. Proc. Symp. on Mathematical aspects of finite elements in partial differential equations, Mathematics Research Center, University of Wisconsin, Madison, April, 1974.
6. M. Crouzeix, Sur l'approximation des équations différentielles opérationnelles par des méthodes de Runge–Kutta. thèse de doctorat d'État Université de Paris VI, 1975.
7. M. Crouzeix and P. A. Raviart, Conforming and non conforming finite elements methods for solving the stationary Stokes equations, *RAIRO* **3** (1974), 33–76.
8. M. Fortin, Utilisation de la méthode des éléments finis en mécanique des fluides. Calcolo XII, fasc. IV, 405–441 and XIII, fasc. 1, 1–20.
9. M. Fortin, Résolution numérique des équations de Navier–Stokes par des éléments finis de type mixte, Rapport de recherche 76-184, IRIA–LABORIA 78–150, Le Chesnay, France.

10. M. FORTIN, R. PEYRET, AND R. TEMAM, Résolution numérique des équations de Navier-Stokes pour un fluide incompressible. *J. Mécanique* **10** (1971), 357–390.
11. R. GLOWINSKI AND PIRONNEAU, Numerical Methods for the first biharmonic equation and for the two-dimensional Stokes problem to appear.
12. C. JOHNSON, On the convergence of a mixed finite element method for plate-bending problems, *Numer. Math.* **21** (1973), 43–62.
13. J. LERAY, Essai sur les mouvements plans d'un liquide visqueux que limitent des parois. *J. Math. Pures Appl.* **13** (1934), 331–418.
14. P. LESAINT, Sur la résolution des systèmes hyperboliques du premier ordre par des méthodes d'éléments finis, Thèse de doctorat d'État Université de Paris VI, 1975.
15. P. LESAINT AND P. A. RAVIART, On a finite element method for solving the mention transport equations, *in* "Mathematical Aspects of Finite Elements in Partial Differential Equations" (C. de Boor, Ed.), pp. 89–123, Academic Press, New York, 1974.
16. J. L. LIONS, "Quelques méthodes de résolution de problèmes aux limites non linéaires," Dunod, Paris, 1969.
17. P. A. RAVIART AND T. M. THOMAS, A mixed finite element method for 2nd order elliptic problems, *in* "Proceedings of the Symposium on the mathematical aspects of the finite element method," Rome, 1975. Lecture Notes in Math., Springer-Verlag, Berlin/New York, 1976.
18. R. TEMAM, "On the theory and numerical analysis of the Navier–Stokes Equations," North–Holland, Amsterdam, 1977.
19. F. THOMASSET, Numerical solution of the Navier–Stokes equations by finite element methods, Rapport 77001, IRIA–LABORIA, Le Chesnay, France.